AAPS Open

RESEARCH Open Access

Sugar molecules as a physical barrier separating therapeutic antibody proteins in freeze-dried formulations: small-angle X-ray scattering insights

Sebastian Groël[1], Ricarda Nagel[1], Jonas Binder[1], Michael Sztucki[2], Wolfgang Frieß[1], Tim Menzen[3], Gerhard Winter[1*] and Evgenyi Shalaev[4*]

Abstract

The paper investigates structure of freeze-dried formulations of a therapeutical monoclonal IgG_1 with non-reducing disaccharides, sucrose and trehalose, as lyoprotectors. Formulations with variable sugar-to-protein ratios are manufactured using different freeze-drying protocols and post-drying temperature treatments. Small-angle X-ray scattering (SAXS) is applied to study packing arrangements of IgG_1 molecules in the crowded solid-state environment. The retention of amorphous structure by the lyoprotectors is confirmed with the simultaneous wide-angle X-ray scattering (WAXS) tests. The new finding is the observation of two IgG_1 SAXS peaks in the crowded environment, with position of one peak (peak A) changing with sugar-to-protein ratio, whereas the second peak (peak B) position is similar in all the formulations tested. The protein center of mass distance, which is calculated from the position of the peak A, increases with the increase in sugar content from 45 Å to 65 Å (sugar-to-protein mass ratio 0.79 to 7.95). Sugar molecules therefore serve as a physical barrier between IgG_1 molecules. While the sugar-to-protein ratio significantly impacts protein separation, other factors, such as disaccharide type, presence of a surfactant, or drying process and post-drying thermal treatment, have minimal effect. The origin of the peak B has not been established yet, with three hypotheses considered. The results highlight applicability of SAXS for quantification of separation distances between protein molecules in freeze-dried formulations, thus improving the fundamental understanding of the stability of protein drugs.

Keywords SAXS, Freeze-drying, Protein, MAb, Solid-state, Protein interaction, Aggregation

*Correspondence:
Gerhard Winter
gerhard.winter@cup.uni-muenchen.de
Evgenyi Shalaev
evgenyi.shalaev@abbvie.com
Full list of author information is available at the end of the article

Graphical Abstract

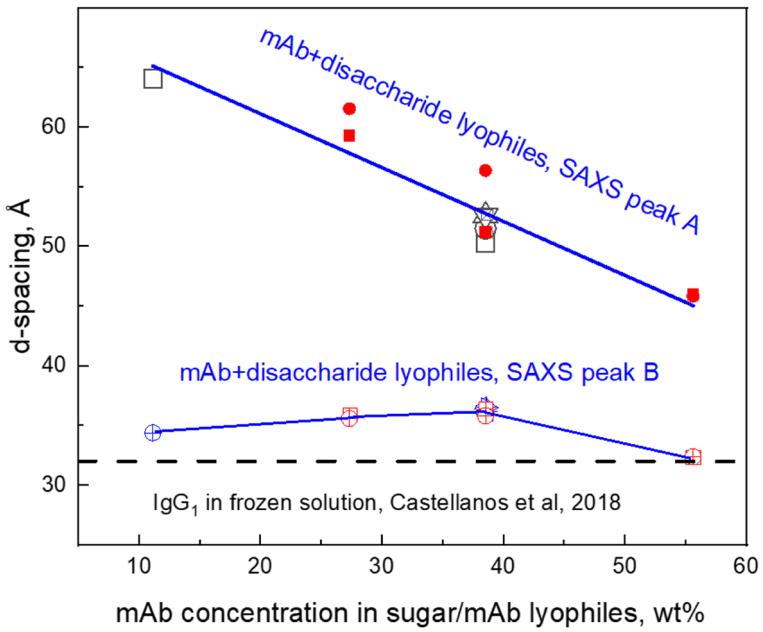

Introduction

Protein drugs are used to treat a broad range of diseases, including e.g., cancer, diabetes, and immunological disorders (Urquhart 2023). While many proteins are sufficiently stable to formulate them as ready-to-use solution, there are also many cases of protein molecules which are insufficiently stable in aqueous solutions (Frokjaer and Otzen 2005). A standard way to improve stability is to remove water by lyophilization (freeze-drying), (Gatlin and Nail 1994). However, freeze-drying itself may also destabilize protein molecules. Therefore, lyoprotectors are used to ensure protein stability during both freeze-drying and storage. The non-reducing disaccharides, sucrose and trehalose, represent the most common lyoprotectors (Izutsu 2018). The sugars may protect proteins via multiple pathways, which are not necessarily exclusive, including water replacement, water entrapment, anchorage, molecular mobility modification, and stabilization of the ionization state of amino acid residues upon dehydration (Arsiccio and Pisano 2018; Lerbret et al. 2012; Cicerone et al. 2015; Hill et al. 2005). In addition to these mechanism, sugars may also provide protection against the most common degradation mechanism, aggregation, by serving as a physical barrier between protein molecules, increasing the distance between protein molecules and preventing close contacts (Chang et al. 1996a; Pérez-Moral et al. 2010; Strickley and Anderson 1997). Protein packing arrangements in crowded environments, including frozen solutions and freeze-dried formulations, has been studied by small-angle X-ray and neutron scattering (SAXS and SANS) methods. In the majority of cases, a single SAXS or SANS peak, which was commonly referred as protein–protein interaction peak, was observed (Curtis et al. 2012a, 2012b; Khodadadi et al. 2014; Castellanos et al. 2018, 2016). The position of the peak corresponds to the center-of-mass distance between protein molecules (Curtis et al. 2012a, 2012b; Phan-Xuan et al. 2020). In several lyophilized formulations of bovine serum albumin (BSA) with disaccharides, two SANS or SAXS peaks were detected (Cristiglio et al. 2024). The two peaks were proposed to originate from two populations of protein molecules with different protein–protein separation distances. Two SAXS & SANS peaks were also observed in a freeze-dried glucose:lysozyme 3:1 (w/w) formulation, whereas disaccharides:lysozyme mixtures all had a single protein peak (Cristiglio et al. 2024).

In this study, we use SAXS to study IgG_1 molecules packing in freeze-dried formulations as a function of disaccharide-to-protein ratio and processing history. Two SAXS peaks are detected in all formulations tested. Position of peak A, which is identified as the protein interaction peak, changes with sugar-to-protein

ratio, while the origin of the second peak, peak B, is uncertain, with three hypotheses proposed. A correlation between sugar-to-protein ratio and protein separation distance, as calculated from the position of SAXS peak A, is observed. Several other formulation and process variables, which are tested in this study, have a minimal impact on the separation distance between protein molecules.

Material and methods

Preparation of formulations

The IgG_1 monoclonal antibody was used as 150 mg/ml stock solution in 20 mM Histidine (Alfa Aesar, Ward Hill, MA, USA) buffer pH 5.5. Sucrose (Sigma-Aldrich, Steinheim, Germany), trehalose (VWR International, Radnor, PA, USA) and polysorbate 20 (Croda, Edison, NJ, USA) were spiked to this solution to get the formulations according to Table 1. The finalized formulations were filtered with a 0.22-µm PES Sartolab® RF vacuum filter unit (Sartorius AG, Goettingen, Germany) and 1 ml of the solutions were filled in 2R vials (MGlas AG, Muennerstadt, Germany). West 13-mm Lyo Nova Pure RS 1356 4023/50 G stoppers were used. Trehalose was obtained from VWR International, Radnor, PA, USA, sucrose from Sigma-Aldrich, Steinheim, Germany and polysorbate 20 (PS20) from Croda, Edison, NJ, USA.

Freeze-drying protocols

The freeze-drying protocols can be found in Supp 1. The conventional cycle (con.) reflects a conservative drying cycle keeping the product temperature below T_g' during primary drying. The collapse drying cycles (col45°C and col55°C) exceed the collapse temperature of the formulations (T_c) during primary drying. The processes 45°C16h and 70°C2h, include a post-drying tempering step 45 °C for 16 h and 70 °C for 2 h, respectively. This process step was executed after freeze-drying with already closed vials and thus is an additional exposure of the samples to elevated temperatures. This should lead to structural relaxation of the amorphous samples which has been connected with increased protein stability (Abdul-Fattah et al. 2007). As this step is referenced as annealing step in the research area of amorphous substances and other publications, the word "tempering" was used instead to clearly distinguish from the "annealing process" in the freezing step of a lyophilization cycle (Luthra et al. 2008; Groël et al. 2023). For the tempering processes, products created by the conservative cycle were used.

Residual water (r.w.)

A coulometric Karl-Fischer Titration was utilized to measure the r.w. of the samples. An Aqua 40.00 Vario plus head space titrator (ECH Elektrochemie Halle GmbH, Halle (Saale)) was used. The lyophilized samples were grounded and partly transferred into a measurement 2R vial under dry nitrogen atmosphere. For structural collapsed samples, 0.5 ml methanol, Dry, Hydranal™

Table 1 Concentration of sugar, surfactant, and protein in the pre-lyophilization solutions and properties of the lyophilized products. See Materials and Methods for samples details. Standard deviations of residual water content and post-lyo aggregates are for n=3.

sample ID	sucrose [g/L]	trehalose [g/L]	ps20 [g/L]	IgG_1 mAb [g/L]	residual water after freeze-drying [%]	T_g	Aggregates pre-lyo [%, peak area]	Aggregates post-lyo [%, peak area]
con_50_ps20_suc	79.45	-	0.4	50	1.05 ± 0.04	72.6	0.33	0.57 ± 0.03
45°C16h_50_ps20_suc	79.45	-	0.4	50	0.98 ± 0.13	77.8		0.62 ± 0.05
70°C2h_50_ps20_suc	79.45	-	0.4	50	1.06 ± 0.00	72.6		0.49 ± 0.06
col45°C_50_ps20_suc	79.45	-	0.4	50	1.01 ± 0.13	78.3		0.50 ± 0.02
col55°C_50_ps20_suc	79.45	-	0.4	50	0.54 ± 0.04	70.5		0.63 ± 0.06
con_50_w/o_suc	79.45	-	-	50	1.00 ± 0.03	74.4	0.33	0.57 ± 0.05
col45°C_50_w/o_suc	79.45	-	-	50	0.88 ± 0.12	80.3		0.52 ± 0.01
con_10_ps20_suc	79.45	-	0.4	10	1.20 ± 0.03	64.3	0.40	0.43 ± 0.05
con_30_tre	-	79.45	0.4	30	0.93 ± 0.05	112.4	0.43	0.24 ± 0.06
con_50_tre	-	79.45	0.4	50	0.81 ± 0.02	108.8	0.41	0.81 ± 0.02
con_100_tre	-	79.45	0.4	100	0.64 ± 0.01	132.2	0.41	0.33 ± 0.04
col45°C_30_tre	-	79.45	0.4	30	3.39 ± 0.08	79.2	0.43	0.22 ± 0.04
col45°C _50_tre	-	79.45	0.4	50	0.70 ± 0.11	116.2	0.41	0.91 ± 0.04
col45°C_100_tre	-	79.45	0.4	100	0.72 ± 0.03	153.0	0.41	0.93 ± 0.04

(Honeywell Chemicals, Charlotte, NC, USA) was added to the measurement vial to extract all water. The vials were heated in an oven (70 °C for methanol containing samples, 100 °C for all other samples) to transfer the water with the gas stream into the measurement cell.

Differential scanning calorimetry and freeze-drying microscopy.

A differential scanning calorimeter Mettler Toledo DSC 821e (Mettler Toledo, Gießen, Germany) was used to determine the values of Tg (glass transition temperature of the freeze-dried formulations) and Tg'. For the T_g of the solids, about 5–15 mg of a freeze-dried sample was transferred to an aluminum crucible in a controlled atmosphere with a humidity < 10%. An empty crucible was used as reference pan and the crucibles were hermetically sealed. A modulated scanning mode was utilized with a heating rate of 2 K/min, a period of 2 min and an amplitude of 1 K. To analyze the data, the obtained curve was extracted in a reversing, non-reversing and total curve. The reversing curve was used to determine the Tg as inflection point of the change in heat capacity.

To determine the T_g' of the Liquid formulations, 10 µl of the sample was transferred to the aluminium crucible and hermitically sealed. The Tg' was then determined by freezing the solution to −50 °C with a cooling rate of 10 K/min. After a hold time of −50 °C for 10 min, the samples were heated with 10 K/min to + 20 °C and the T_g' was determined from the heating curve as inflection point of the heat capacity.

The collapse temperature of the formulations was investigated using an optical Olympus BX53M microscope combined with a Linkam stage. 3 µl of the liquid sample was pipette on the sample holder and frozen to −45 °C. The temperature was ramped with 0.1 °C/min and the collapse temperature determined when the first ruptures in the solid matrix were observable.

Size Exclusion Chromatography (SEC)

IgG_1 aggregation before and after freeze-drying was measured by SEC. Separation was conducted with a Waters 2695 Separation Module (Waters GmbH, Eschborn, Germany). To determine the content of soluble aggregates a Tosoh TSKgel G3000 SWXL column (Tosoh Bioscience, Griesheim, Germany) was utilized applying a flowrate of 1 ml/min. The elution buffer consists of 100 mM sodium phosphate pH 7.0 containing 200 mM sodium chloride. A Waters 2487 Dual λ Absorbance Detector (Waters) at the wavelength of 280 nm was used for detection. For the 2 g/l formulations, 20 µl reconstituted sample was injected, whereas formulations with higher protein concentrations were diluted to a concentration of 5 g/l and 10 µl were injected. To determine the amount of aggregates, the area in mAU of the monomeric protein peak as well as the higher molecular weight species (protein aggregates) were integrated. The area of the protein aggregates was then expressed as percentage area in relation to the total peak area.

Small and wide-Angle X-Ray Scattering

SAXS/WAXS experiments were conducted at the ID02 beamline of the European Synchrotron Radiation Facility, Grenoble, France (Narayanan et al. 2022) using an X-ray energy of 1Å. The detector was a Eiger2X 4M pixel detector (Dectris) at a sample to detector distance of 1 m for SAXS and a RayoniX LX 170HS ccd camera at a sample to detector distance of 120 mm for WAXS. The 2D scattering images were normalized to absolute units and azimuthally averaged using standard procedures. The samples were quickly transferred to capillaries of 1.5 mm diameter (Hilgenberg, Malsfeld, Germany) to avoid water absorption and sealed for the measurements. A mass of approximately 20 mg was sampled by introducing a glass capillary top-to-bottom into the intact lyophilizate at multiple locations of the vial. During this, the lyophilizate in the capillary was gently compressed to ensure an adequate scattering signal from the sample. 10 images were recorded along the capillary and averaged to improve statistics. The instrumental background and scattering of an empty capillary were subtracted.

Position of the peaks was determined by fitting a polynomial function of the 5th order in the log–log-plot to the measured SAXS curves and using the respective maximum values fitted (fitting example in Supp. 5). A power law was utilized to fit the scattering in the low q region. The distance between the proteins was calculated from the q according to Eq. 1.

$$d = \frac{2\pi}{q} \tag{1}$$

Results

The water content of the majority of samples is determined to be between 0.5 to 1.6 wt %, with one sample having a higher water content of 3.4 wt% (Table 1). In the group of the sucrose samples containing 50 g/l protein only one sample (col55°C_50_ps20_suc) differs more than 0.1% in value from the other samples. The trehalose samples have residual water content less than 1 wt%, with the single exception of one of the collapsed trehalose sample (col45°C_30_tre) with 3.4 wt % water. All formulations are amorphous, based on the WAXS data (representative WAXS patterns are provided in Supp. 3). Most freeze-dried samples have slightly higher level of aggregates as compared to solutions prior lyophilization, with the maximal difference of 0.5% for 3

trehalose formulations (Table 1). In two of the formulations (con_30_tre and con_100_tre) post-lyo aggregates level was slightly lower than pre-lyo. Overall, strong formulation- and manufacturing process-related trends are not observed for the protein aggregation by SEC and residual water content data. Detailed information of the specific surface area of the lyophilized cakes can be accessed in the supplementary material. The surface area provides information about the microscopic structure of the cake and indicates through a decrease in specific surface area the successful rupture of the structure of the samples that are described as collapsed.

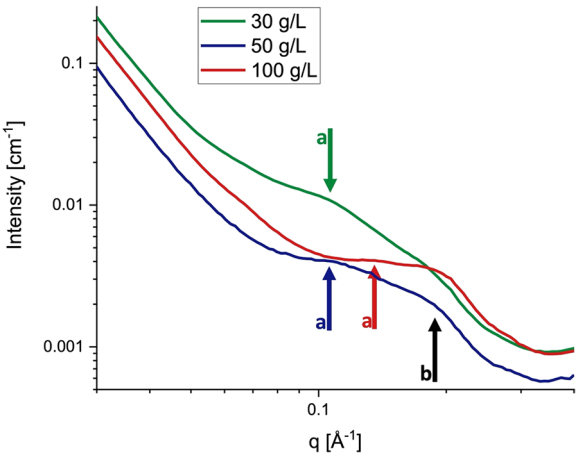

Fig. 1 SAXS patterns of freeze-dried samples with different IgG_1 concentration in the presence of 79.45 g/l trehalose (corresponding sugar-to-protein ratios of 2.65 in green, 1.59 in blue and 0.79 in red). Arrows indicate the peak regions

Representative SAXS curves for mAb formulations with different trehalose-to-protein ratios are presented in Fig. 1. Scattering intensity in the low-angle scattering region ($q < 0.05$ Å^{-1}) follows the power law exponent function with the slope (p, Porod invariant) equal to 4. A Porod invariant value of 4, which indicates scattering structures with well-defined sharp interfaces (Narayanan et al. 2008), is typical for freeze-dried formulations with porous morphology with extensive air/solid interfaces (Phan-Xuan et al. 2020; Cristiglio et al. 2022).

Two broad overlapping peaks are observed in the higher-angle scattering region. In the 100 mg/ml samples (lowest trehalose:mAb w/w ratio of 0.8:1), peak A is shifted to higher q, as compared to formulations with higher trehalose-protein ratio. The d-spacing for peak A increases from 46 Å to 59 Å with sugar/protein ratio increase from 0.8 to 2.65 (Table 2). The position of peak B, at $q \sim 0.18$ Å^{-1} (d-spacing ~ 35 Å), is similar for the formulations with different trehalose-to-mAb ratio, with d-spacing differences of 4 Å or less (Table 2). The same trend is observed for sucrose formulations; the increase in sucrose/protein ratio from 1.6:1 to 8:1 (50 and 10 g/l mAb, respectively) results in the shift of the peak A to lower q (higher d-spacing) while the peak B position is essentially ratio independent (Table 2). In the formulation with 40:1 sucrose-to-protein ratio (2 g/l mAb), protein interaction peaks are not detected in the SAXS patterns, probably because of very low protein concentration (Supp. 4b).

Table 2 Position of the protein interaction peaks, q, obtained by fitting the SAXS curves, and corresponding d = spacing values (Eq. 1). See Materials and Methods for samples details including freeze-drying conditions (conservative cycle and cycle with collapse) and post-drying tempering (annealing) treatment (sample names starting with 45 °C and 70 °C)

Sample	Sugar/Protein ratio [#]	peak A, q, [Å^{-1}]	peak B, q, [Å^{-1}]	peak A, d [Å]	peak B, d [Å]
con_50_ps20_suc	1.59	0.1240	0.1735	50.7	36.2
45°C16h_50_ps20_suc	1.59	0.1249	0.1725	50.3	36.4
70°C2h_50_ps20_suc	1.59	0.1220	0.1726	51.5	36.4
col45°C_50_ps20_suc	1.59	0.1195	0.1736	52.6	36.2
col55°C_50_ps20_suc	1.59	0.11952	0.1721	52.6	36.5
con_50_w/o_suc	1.59	0.1193	0.1736	52.7	36.2
col45°C_50_w/o_suc	1.59	0.1205	0.1721	51.2	36.5
con_10_ps20_suc	7.95	0.0981	0.1954	64.1	34.4
con_30_tre	2.65	0.1060	0.1750	59.3	35.9
con_50_tre	1.59	0.1229	0.1725	51.2	36.4
con_100_tre	0.79	0.1367	0.1940	46.0	32.4
col45°C_30_tre	2.65	0.1021	0.1765	61.6	35.6
col45°C _50_tre	1.59	0.1146	0.1754	56.4	35.8
col45°C_100_tre	0.79	0.1371	0.1940	45.8	32.4

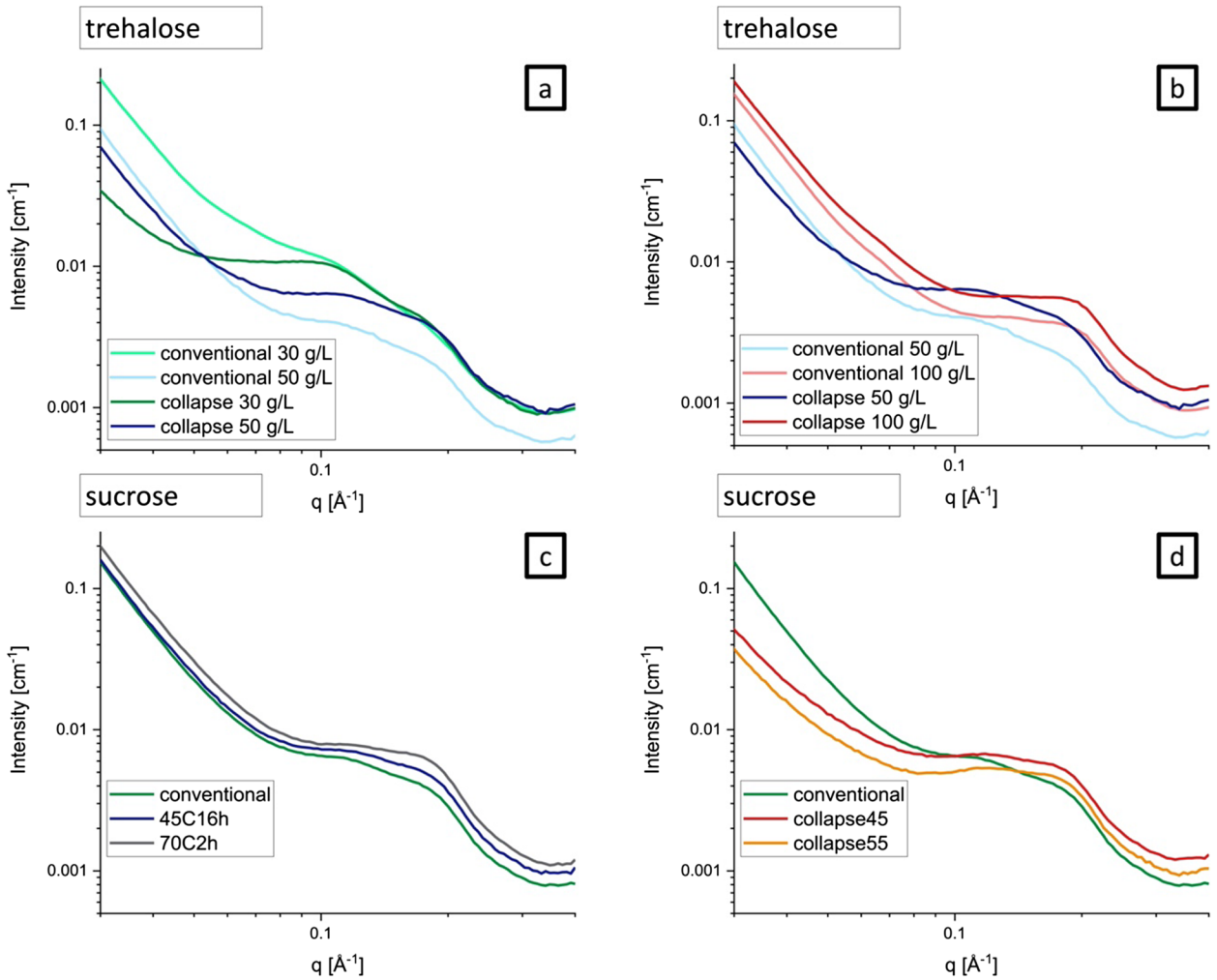

Fig. 2 Protein interaction peaks in SAXS patterns of freeze-dried IgG_1 formulations at different sugar to protein ratios (corresponding 2.65 for 30 g/l, 1.59 for 50 g/l and 0.79 for 100 g/l) and processing conditions. a) and b) trehalose matrix processed conventional or with collapse with protein concentrations from 30 g/L to 100 g/L. c) and d) sucrose matrix 50 g/L processed with 5 different freeze-drying conditions. Examples of complete SAXS curves are provided in in Supp. 3 to demonstrate that lower q scattering slope is similar between different formulations

Exemplary SAXS curves for samples with different processing history, including intentional collapse during primary drying and post-drying annealing, are shown in Fig. 2. Post-drying temperature treatment (45°C/16h and 70°C/2h) does not result in a noticeable change in the positions of both SAXS peaks.

The SAXS results are summarized in Table 2 and Fig. 3, which demonstrates that the position of peak B is essentially constant (within 4 Å) between formulations tested, while the d-spacing for peak A increases with the increase in the sugar-to-protein ratio. Manufacturing history does not have a major impact on either peak A or B, although in collapsed PS20-containing sucrose 50 g/l and trehalose 30 g/l and 50 g/l formulations, a minor d-spacing shift from 2 to 5 Å for peak A is observed.

Exchanging trehalose against sucrose does not impact the overall SAXS curve appearance (two protein peaks), the low-angle portion of the SAXS region (Fig. 4), and the peaks' positions (Fig. 4, Table 2). Furthermore, formulations prepared with and without PS20 have similar SAXS patterns (Supp. 5) and peaks positions (Table 2, Fig. 3).

Discussion

Protein–protein interactions in crowded environment, such as in frozen solutions and freeze-dried materials, have been studied by SAXS and SANS, with both methods providing comparable results (Curtis et al. 2012a, 2012b; Castellanos et al. 2018, 2016; Cristiglio et al. 2022, 2024). Freezing of protein solutions removes the majority of water in the form of ice crystals, with water content

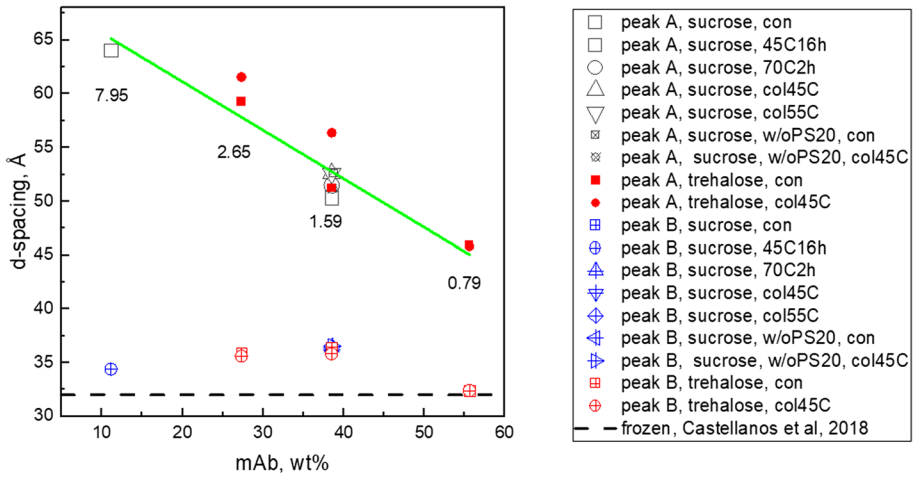

Fig. 3 d-spacing of two protein interaction peaks in freeze-dried sugar-IgG formulations. The horizontal line represents IgG_1 center-of-mass distances in frozen solution, from (Castellanos et al. 2018). Empirical linear regression line for peak A (green) is provided as visual aid. The mAb wt percents in the freeze-dried formulations are calculated based on the amounts of the protein, lyoprotector, and surfactant in the pre-lyophilization solutions, while residual water and buffer are not included in the calculation. Numbers the graph indicate sugar/protein wt ratios

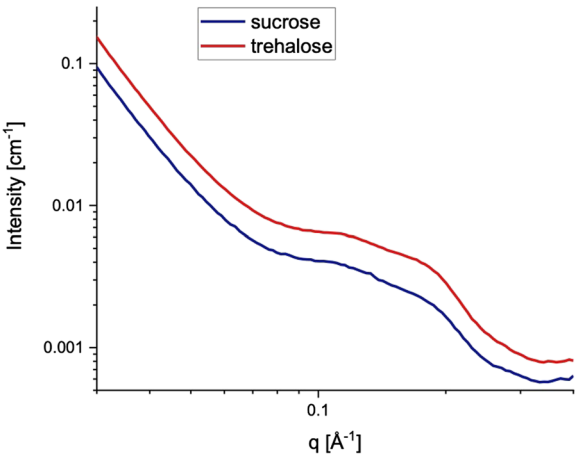

Fig. 4 SAXS patterns of freeze-dried formulations prepared from 50 g/L mab solution formulated with sucrose (blue curve) or trehalose (red curve) matrix at sugar-to-protein weight ratio 1.59 to 1 (formulations con_50_ps20_suc and con_50_tre from Table 1)

in the freeze-concentrated amorphous phase estimated to be approx. 20 wt% (Buera et al. 2011; Panagopoulou et al. 2011), while freeze-dried protein formulations typically contain less than 5 wt% water. SAXS/SANS patterns of these systems usually have a broad peak, which position, when expressed in d-spacing scale, corresponds to center-of-mass distance between protein molecules (Castellanos et al. 2017). While the majority of SANS and SAXS studies of proteins in the crowded environment has been performed with lysozyme, there are also several reports on IgG (Castellanos et al. 2018, 2016). In those studies, SANS patterns were obtained for frozen, cryoprotector-free, mAb solutions, and the SANS peak, at $q \sim 0.2\ A^{-1}$, was assigned to be protein interaction peak in the freeze-concentrated phase (Castellanos et al. 2018, 2016). The position of the protein interaction peak in frozen solutions was reported at d-spacing of approx. 32 Å for IgG_1 in 25 mM histidine buffer at pD 6.4 and at 31 Å in 10 mM sodium acetate buffer at pD 5.6 (Castellanos et al. 2018, 2016). These proteins center-of-mass distances, dm, are less than the radius of gyration, Rg, for IgG_1 which was reported to be 60 Å in solution ($dm \sim 2Rg/3$) (Kilár et al. 1985). It was proposed that such short protein–protein distances are caused by interdigitation of molecules of antibodies in crowded environments, as the result of their flexibility and non-globular structure (Castellanos et al. 2018, 2016).

In the present study, two peaks are observed in the SAXS patterns of freeze-dried IgG_1 formulations (Fig. 1, 2, 4). Position of peak B, at approx. 32 to 36 Å, is similar between formulations, whereas peak A shifts consistently with increase in sugar-to-protein ratio from 46 Å to 64 Å (Fig. 3, Table 2). Physical origin of peak B is discussed later in this section, while peak A corresponds to protein molecules which are separated by sugar molecules, with the protein–protein separation distance increasing with the increase in sugar-to-protein ratio. The d-spacings for peak A are similar between sucrose and trehalose formulations. This corresponds to results reported for freeze-dried formulations of lysozyme and BSA with these two disaccharides (Cristiglio et al. 2022, 2024). Inclusion of PS20 in sucrose formulations does not have any major impact on d-spacing (Fig. 3, Table 2). Formulation with PS20 has similar, yet slightly lower (by 2 Å) d-spacing

than corresponding PS20-free formulation (50.7 Å vs 52.7 Å, Table 2). This observation of similar protein–protein distances in freeze-dried formulations with and without PS20 is consistent with the report on frozen solutions of lysozyme (Yuan et al. 2023). The fact that the protein–protein distance is similar in formulations with and without surfactant suggests that PS20's protective role may not be connected with physical separation of protein molecules, instead arising from reducing shear stress during freezing step of the lyophilization process or reconstitution of the dried product, e.g., by saturating interfaces and/or forming molecular complexes with protein (Singh et al. 2017; Chang et al. 1996b; Lee et al. 2011; Li et al. 2019; Zhang et al. 1995, 1996). Impact of post-drying thermal treatment (tempering) on the protein separation distance is also minimal (Table 2). The large scale molecular motions are expected to be arrested in the freeze-dried samples, as the tempering temperature is well below the calorimetric T_g (Table 1). The positioning of the protein molecules become "fixed" mainly during the freezing step of the freeze-drying process and is not affected by the tempering. Collapse during freeze-drying, on the other hand, may have an impact on protein–protein separation distance, as above T_g' protein molecules are more mobile and molecular rearrangements are possible. Several collapsed formulations, including sucrose 50 g/l and trehalose 30 and 50 g/l formulations with PS20 (sugar/protein ratios of 1.6 and 2.65), have slightly higher protein–protein distances, by 2 to 5 Å, as compared with the non-collapsed samples (Table 2). The increased protein separation in the collapsed systems may reduce the aggregation propensity and contribute to a better long term stability. Improved stability of collapsed formulations was reported in several studies (Groël et al. 2023; Schersch et al. 2010, 2012) although the relatively minor increase in protein separation in collapsed formulations might not be a main mechanism for the stability improvement. Note also that for the formulation with the higher protein content (100 g/l trehalose formulation, sugar/protein ratio 0.79), collapsed and non-collapsed samples have essentially identical d-spacing, with 45.8 and 46.0 Å, respectively. To ultimately answer the question whether the impact of collapse on protein–protein distance may depend on the sugar/protein ratio, additional studies are needed.

The origin of peak B is less certain, with three hypothesis are considered herein.

Hypothesis 1. This hypothesis is based on the similarity in the position of peak B to the protein interaction peak which was observed in frozen, cryoprotector-free, mAb solutions, which was proposed to originate from interdigitated mAb molecules. (Castellanos et al. 2018, 2016) Accordingly, peak B in the freeze-dried formulations can correspond to tightly packed, and interdigitated, IgG_1 molecules, without lyoprotector molecules present between them. Under this interpretation, detection of two SAXS peaks would indicate two IgG1 populations, one with protein molecules physically separated from each other by sugar molecules (peak A) and another with close protein–protein contacts (peak B). A possible physical mechanism for formation of two populations of protein molecules during freeze-drying is proposed in Supplemental materials (Supp. 8). If the two-population hypothesis is confirmed in future studies, it could have a significant practical relevance. In addition to the different distances between the proteins, the two populations of IgG1 molecules would also have different microenvironment, which could result in different rates of chemical degradative processes, such as deamidation and oxidation. Note that heterogeneity in protein distribution between surface and bulk was reported for various dried formulations, with protein molecules located at either air/solid interface (which was operationally defined as within 10 nm from the interface) or in the bulk (Wilson et al. 2020; Xu et al. 2014). The surface-exposed and bulk protein molecules had different stability profiles, with the degradation rate for the surface-located molecules been higher by an order of magnitude, as reported in a study of stability of freeze-dried formulations of human growth hormone (Xu et al. 2014). Separation of protein molecules from lyoprotector in freeze-dried formulations was also observed using Raman mapping method (Padilla et al. 2011; Forney-Stevens et al. 2014).

This first hypothesis is based on the concept of tightly packed, and interdigitated, IgG molecules, with the center-of-mass distance significantly lower than the radius of gyration (dm ~ 35 Å *vs* Rg ~ 60 Å), which is not intuitive, and therefore two additional explanations are considered, as Hypothesis 2 and Hypothesis 3.

Hypothesis 2. According this hypothesis, both SAXS peaks A and B originate from the competition of the short-range attraction and a longer-range repulsion between the same IgG molecules (Liu et al. 2005). The short-range attractive potential is expected to dominate and a change of the weaker long-range repulsion hardly affects the potential form close to the particle. Therefore, the interaction at small q values (peak A) responds to the change of the repulsion range and is sensitive to a change of the sugar to protein ratio. Peak B represents the invariant short-range

attraction between the molecules in the crowded environment and is observed at the same q value for all samples. This suggests that the presence of sugar, at the sugar-to-protein ratios studied here, does not impact the short-range attractive interaction between IgG1 molecules in freeze-dried formulations. Note also that d-spacings for both Peak A (45 to 60 Å) and Peak B (35 Å) are shorter than 2Rg for IgG1 molecules in aqueous solution (60*2 = 120 Å), which implies significant changes in the shape and dimensions of IgG1 molecules when aqueous solution is converted into a solid dehydrated form.

Hypothesis 3. Peak B could be interpreted as the form factor resulting from scattering of individual IgG molecules, rather than from intermolecular interactions. However, the scattering from individual protein molecules is usually detected in dilute aqueous solutions, where the electron density contrast between protein and solvent molecules is well defined. Such conditions are different from crowded environment in frozen protein solutions and freeze-dried powders with strong interparticle interaction (Curtis et al. 2012b; Khodadadi et al. 2014; Castellanos et al. 2018, 2016; Phan-Xuan et al. 2020), which makes it more difficult to measure the form factor under these conditions.

The data do not allow a definite conclusion on the nature of the SAXS peak B, and additional studies are needed to distinguish between the interpretations proposed. Note that both interpretations (1) and (2) imply that there are close intermolecular interactions between IgG_1 molecules. The absence of any significant amounts of IgG1 aggregates in the reconstituted solutions (Table 1) indicates that attractive protein–protein interactions and/or interdigitation of IgG1 molecules in the freeze-dried material may represent necessary but not a sufficient condition for aggregation which is detected after reconstitution of freeze-dried formulations. Other factors, including preservation of protein higher order structure and H-bonding between lyoprotector and proteins may also play major role in stabilization of proteins against aggregation.

Conclusion

Monitoring position of protein interaction peak in freeze-dried sugar-to-protein formulations allows to assess impact of sugar on physical separation of protein molecules. An important insight of this study is a finding of direct relationship between sugar-to-protein ratio and distance between molecules of IgG_1 in freeze-dried formulations, which is calculated from the position of SAXS peak A, with the distance increasing at higher ratios. This observation aligns with published studies on improved protein stability at higher sugar concentrations. (Xu et al. 2014; Wang et al. 2009) Other formulation and processing factors, such as intentional collapse during primary drying, post-drying annealing, type of disaccharide, and addition of surfactant (PS20) had a minimal impact on the separation distance between protein molecules. Note that some tentative observations, such as a minor difference in the protein interaction peak d-spacing between formulations with *vs* without PS20, and a different response to collapse in a trehalose formulation with a lower sugar/protein ratio, could be of interest for future studies.

The detection of a second peak, peak B, in the SAXS patterns of freeze-dried IgG1 formulations represents another significant result. Position of peak B is similar between the formulations and independent of the sugar-to-protein ratio, in clear contrast to peak A. Three alternative interpretations may explain the physical nature of peak B, i.e., a "second population consisting of interdigitated IgG1 molecules", "short-range attraction between the IgG_1 molecules in the crowded environment", and "form factor of isolated IgG_1 molecules". The two former hypotheses are based on SANS studies of frozen IgG solutions and SAXS/SANS studies of concentrated lysozyme solutions, respectively (Castellanos et al. 2018, 2016; Shukla et al. 2008). Note that either hypothesis indicates the existence of interacting protein molecules in the lyophiles, with the interaction to be essentially independent of sugar-to-protein ratio. The latter hypothesis is a new suggestion, as the analysis of the protein form factor in crowded environment has not been proposed in previous investigations. The data available do not allow to prove which one of the hypotheses is correct. To address the origin of the SAXS peak B in IgG/sugar lyophiles, a follow-up study of lyoprotector-and-protein system is warranted. In particular, future investigation should address a data gap between frozen cryoprotector-free IgG solutions (single SAXS peak) and the present study where two protein peaks are observed in freeze-dried IgG/disaccharide mixtures. Inclusion of freeze-dried formulations with higher protein-to-sugar ratios could also provide an input into interpretation of the SAXS results, as illustrated graphically in Supp. 7. Future studies may further benefit from a contrast variation approach which is standard for SANS (Castellanos et al. 2017) and could also be utilized in SAXS (Tokuda et al. 2016). However, the latter would be more complex because difference in electron density for SAXS experiments are relatively lower than contrast in scattering length between H and D in SANS.

Lastly, further investigation into the effects of different freeze-drying steps, particularly the impact of

freezing rates on protein and protein–sugar interactions, could yield deeper insights into optimizing formulation stability.

Supplementary Information

The online version contains supplementary material available at https://doi.org/10.1186/s41120-025-00120-8.

Supplementary Material 1.

Disclaimer

ES is an employee of AbbVie. He participated in design of the study, in the analysis and interpretation of data, and in writing, reviewing, and approval of the publication. Abbvie did not provide financial support for the study.
TM is an employee of Coriolis Pharma. He participated in design of the study, reviewing, and approval of the publication. Coriolis Pharma did not provide financial support for the study.

Authors' contributions

SG: Conceptualization, Data curation, Formal analysis, Investigation, Methodology, Visualization, Writing – original draft/review & editing. RN: Formal analysis, Investigation, Writing – review & editing. JB: Investigation, Writing – review & editing. MS: Formal analysis, Investigation, Resources, Writing – review & editing. WF: Methodology, Resources, Writing – review & editing. TM: Conceptualization, Methodology, Writing – review & editing. GW: Conceptualization, Methodology, Project administration, Resources, Supervision, Writing – review & editing, Funding Acquisition. ES: Conceptualization, Data curation, Formal analysis, Methodology, Visualization, Project administration, Supervision, Writing – original draft/review & editing. All authors read and approved the final manuscript.

Funding

Open Access funding enabled and organized by Projekt DEAL.

Declarations

Data availability

Data can be provided on request.

Competing interests

Not applicable.

Funding

Not applicable.

Acknowledgements

The authors acknowledge the ESRF for the provision of Synchrotron Radiation Facilities under the proposals LS-2993 and LS-3210. Further thank to Alice Hirschmann and Katharina Prüßmann for their continuous support and administrative efforts, Bakul Bhatnagar for initial discussions on ESRF study design, and T Narayanan for helpful inputs on interpretation of SAXS data.

Author details

[1]Department of Pharmacy, Center for Drug Research, Ludwig-Maximilians-Universität München, Munich, Germany. [2]European Synchrotron Radiation Facility, CS 40220, Grenoble, Cedex 9 38043, France. [3]Coriolis Pharma Research GmbH, Fraunhoferstraße 18B, Martinsried 82152, Germany. [4]Development Sciences, Abbvie, Irvine, CA, USA.

Received: 25 March 2025 Accepted: 11 July 2025
Published online: 29 September 2025

References

Abdul-Fattah AM, Dellerman KM, Bogner RH, Pikal MJ (2007) The Effect of Annealing on the Stability of Amorphous Solids: Chemical Stability of Freeze-Dried Moxalactam. J Pharm Sci 96:1237–1250
Arsiccio A, Pisano R (2018) Water entrapment and structure ordering as protection mechanisms for protein structural preservation. J Chem Phys 148:055102
Buera MP, Roos Y, Levine H, Slade L, Corti HR, Reid DS, Auffret T, Angell CA (2011) State diagrams for improving processing and storage of foods, biological materials, and pharmaceuticals (IUPAC Technical Report). Pure Appl Chem 83:1567–1617
Castellanos MM, Clark NJ, Watson MC, Krueger S, McAuley A, Curtis JE (2016) Role of molecular flexibility and colloidal descriptions of proteins in crowded environments from small-angle scattering. J Phys Chem B 120:12511–12518
Castellanos MM, McAuley A, Curtis JE (2017) Investigating structure and dynamics of proteins in amorphous phases using neutron scattering. Comput Struct Biotechnol J 15:117–130
Castellanos MM, Mattison K, Krueger S, Curtis JE (2018) Characterization of the NISTmAb reference material using small-angle scattering and molecular simulation: Part II: concentrated protein solutions. Anal Bioanal Chem 410:2161–2171
Chang BS, Reeder G, Carpenter JF (1996a) Development of a stable freeze-dried formulation of recombinant human interleukin-1 receptor antagonist. Pharm Res 13:243–249
Chang BS, Kendrick BS, Carpenter JF (1996b) Surface-induced denaturation of proteins during freezing and its inhibition by surfactants. J Pharm Sci 85:1325–1330
Cicerone MT, Pikal MJ, Qian KK (2015) Stabilization of proteins in solid form. Adv Drug Deliv Rev 93:14–24
Cristiglio V, Sztucki M, Wu C, Shalaev E (2022) Impact of lyoprotectors on protein-protein separation in the solid state: neutron- and X-ray-scattering investigation. Biochim Biophys Acta BBA - Gen Subj 1866:130101
Cristiglio V, Feng S, Sztucki M, Yuan X, Shalaev E (2024) Two populations of protein molecules detected by small-angle neutron and X-ray scattering (SANS and SAXS) in lyophilized protein:lyoprotector (disaccharide) systems. Soft Matter 20:3897–3900
Curtis JE, Nanda H, Khodadadi S, Cicerone M, Lee HJ, McAuley A, Krueger S (2012a) Small-angle neutron scattering study of protein crowding in liquid and solid phases: lysozyme in aqueous solution, frozen solution, and carbohydrate powders. J Phys Chem B 116:9653–9667
Curtis JE, McAuley A, Nanda H, Krueger S (2012b) Protein structure and interactions in the solid state studied by small-angle neutron scattering. Faraday Discuss 158:285
Forney-Stevens KM, Pelletier MJ, Shalaev EY, Pikal MJ, Bogner RH (2014) Optimization of a raman microscopy technique to efficiently detect amorphous-amorphous phase separation in freeze-dried protein formulations. J Pharm Sci 103:2749–2758
Frokjaer S, Otzen DE (2005) Protein drug stability: a formulation challenge. Nat Rev Drug Discov 4:298–306
Gatlin, LA, Nail SL (1994) Freeze Drying: A Practical Overview. Protein Purif Process Eng. Bioprocess Technology 18: 317–367
Groël S, Menzen T, Winter G (2023) Possibilities and limitations of α-relaxation data of amorphous freeze-dried cakes to predict long term IgG1 antibody stability. Int J Pharm. https://doi.org/10.1016/j.ijpharm.2023.123445
Hill JJ, Shalaev EY, Zografi G (2005) Thermodynamic and dynamic factors involved in the stability of native protein structure in amorphous solids in relation to levels of hydration. J Pharm Sci 94:1636–1667
Izutsu K (2018) Applications of Freezing and Freeze-Drying in Pharmaceutical Formulations. In: Iwaya-Inoue M, Sakurai M, Uemura M (eds) Survive Strategy. Extreme Cold Desiccation. Springer, Singapore, pp 371–383
Khodadadi S, Clark NJ, McAuley A, Cristiglio V, Curtis JE, Shalaev EY, Krueger S (2014) Influence of sorbitol on protein crowding in solution and freeze-concentrated phases. Soft Matter 10:4056–4060
Kilár F, Simon I, Lakatos S, Vonderviszt F, Medgyesi GA, Závodszky P (1985) Conformation of human IgG subclasses in solution: small-angle X-ray scattering and hydrodynamic studies. Eur J Biochem 147:17–25
Lee HJ, McAuley A, Schilke KF, McGuire J (2011) Molecular origins of surfactant-mediated stabilization of protein drugs. Adv Drug Deliv Rev 63:1160–1171

Lerbret A, Affouard F, Hédoux A, Krenzlin S, Siepmann J, Bellissent-Funel M-C, Descamps M (2012) How strongly does trehalose interact with lysozyme in the solid state? Insights from molecular dynamics simulation and inelastic neutron scattering. J Phys Chem B 116:11103–11116
Li J, Krause ME, Chen X et al (2019) Interfacial stress in the development of biologics: fundamental understanding, current practice, and future perspective. AAPS J 21:44
Liu Y, Chen W-R, Chen S-H (2005) Cluster formation in two-Yukawa fluids. J Chem Phys 122:044507
Luthra SA, Hodge IM, Utz M, Pikal MJ (2008) Correlation of annealing with chemical stability in lyophilized pharmaceutical glasses. J Pharm Sci 97:5240–5251
Narayanan T (2008) Synchrotron Small-Angle X-Ray Scattering. In: Borsali R, Pecora R (eds) Soft Matter Charact. Springer, Netherlands, Dordrecht, pp 899–952
Narayanan T, Sztucki M, Zinn T, Kieffer J, Homms-Puron A, Gorini J, Van Vaerenbergh P, Boesecke P (2022) Performance of the time-resolved ultra-small-angle X-ray scattering beamline with the extremely brilliant source. J Appl Crystallogr 55:98–111
Padilla AM, Pikal MJ, Padilla AM (2011) The study of phase separation in amorphous freeze-dried systems, Part 2: investigation of raman mapping as a tool for studying amorphous phase separation in freeze-dried protein formulations. J Pharm Sci 100:1467–1474
Panagopoulou A, Kyritsis A, Sabater I, Serra R, Gómez Ribelles JL, Shinyashiki N, Pissis P (2011) Glass transition and dynamics in BSA–water mixtures over wide ranges of composition studied by thermal and dielectric techniques. Biochim Biophys Acta BBA - Proteins Proteomics 1814:1984–1996
Pérez-Moral N, Adnet C, Noel TR, Parker R (2010) Characterization of the rate of thermally-induced aggregation of β-lactoglobulin and its trehalose mixtures in the glass state. Biomacromolecules 11:2985–2992
Phan-Xuan T, Bogdanova E, Millqvist Fureby A, Fransson J, Terry AE, Kocherbitov V (2020) Hydration-induced structural changes in the solid state of protein: a SAXS/WAXS study on lysozyme. Mol Pharm 17:3246–3258
Schersch K, Betz O, Garidel P, Muehlau S, Bassarab S, Winter G (2010) Systematic investigation of the effect of lyophilizate collapse on pharmaceutically relevant proteins I: stability after freeze-drying. J Pharm Sci 99:2256–2278
Schersch K, Betz O, Garidel P, Muehlau S, Bassarab S, Winter G (2012) Systematic investigation of the effect of lyophilizate collapse on pharmaceutically relevant proteins, part 2: stability during storage at elevated temperatures. J Pharm Sci 101:2288–2306
Shukla A, Mylonas E, Di Cola E, Finet S, Timmins P, Narayanan T, Svergun DI (2008) Absence of equilibrium cluster phase in concentrated lysozyme solutions. Proc Natl Acad Sci 105:5075–5080
Singh SM, Bandi S, Jones DNM, Mallela KMG (2017) Effect of polysorbate 20 and polysorbate 80 on the higher-order structure of a monoclonal antibody and its Fab and Fc fragments probed using 2D nuclear magnetic resonance spectroscopy. J Pharm Sci 106:3486–3498
Strickley RG, Anderson BD (1997) Solid-state stability of human insulin II. effect of water on reactive intermediate partitioning in lyophiles from pH 2–5 solutions: stabilization against covalent dimer formation. J Pharm Sci 86:645–653
Tokuda JM, Pabit SA, Pollack L (2016) Protein–DNA and ion–DNA interactions revealed through contrast variation SAXS. Biophys Rev 8:139–149
Urquhart L (2023) FDA new drug approvals in Q1 2023. Nat Rev Drug Discov 22:346–346
Wang B, Tchessalov S, Cicerone MT, Warne NW, Pikal MJ (2009) Impact of sucrose level on storage stability of proteins in freeze-dried solids: II. Correlation of aggregation rate with protein structure and molecular mobility. J Pharm Sci 98:3145–3166
Wilson NE, Mutukuri TT, Zemlyanov DY, Taylor LS, Topp EM, Zhou QT (2020) Surface composition and formulation heterogeneity of protein solids produced by spray drying. Pharm Res 37:14
Xu Y, Grobelny P, Von Allmen A, Knudson K, Pikal M, Carpenter JF, Randolph TW (2014) Protein quantity on the air-solid interface determines degradation rates of human growth hormone in lyophilized samples. J Pharm Sci 103:1356–1366
Yuan X, Krueger S, Shalaev E (2023) Protein-surfactant and protein-protein interactions during freeze and thaw: a small-angle neutron scattering study of lysozyme solutions with polysorbate and poloxamer. J Pharm Sci 112:76–82
Zhang MZ, Wen J, Arakawa T, Prestrelski SJ (1995) A new strategy for enhancing the stability of lyophilized protein: the effect of the reconstitution medium on keratinocyte growth factor. Pharm Res 12:1447–1452
Zhang MZ, Pikal K, Nguyen T, Arakawa T, Prestrelski SJ (1996) The effect of the reconstitution medium on aggregation of lyophilized recombinant interleukin-2 and ribonuclease A. Pharm Res 13:643–646

Publisher's Note